



Society of Petroleum Engineers

SPE-194350-MS

Evolving Completion Designs to Optimize Well Productivity from a Low Permeability Oil Sandstone Turner Reservoir in the Powder River Basin—One Operator's Experience

Karn Agarwal, Liberty Oilfield Services; Justin Kegel and Bryce Ballard, Ballard Petroleum, LLC; Ely Lolon, Michael Mayerhofer, Leen Weijers, Howard Melcher, Sarah Compton, and Paul Turner, Liberty Oilfield Services

Copyright 2019, Society of Petroleum Engineers

This paper was prepared for presentation at the SPE Hydraulic Fracturing Technology Conference and Exhibition held in The Woodlands, Texas, USA, 5-7 February 2019.

This paper was selected for presentation by an SPE program committee following review of information contained in an abstract submitted by the author(s). Contents of the paper have not been reviewed by the Society of Petroleum Engineers and are subject to correction by the author(s). The material does not necessarily reflect any position of the Society of Petroleum Engineers, its officers, or members. Electronic reproduction, distribution, or storage of any part of this paper without the written consent of the Society of Petroleum Engineers is prohibited. Permission to reproduce in print is restricted to an abstract of not more than 300 words; illustrations may not be copied. The abstract must contain conspicuous acknowledgment of SPE copyright.

Abstract

As the Powder River Basin (PRB) development continues and more wells are drilled, identifying best completion practices is critical to economic success. This operator has completed several Turner horizontal wells drilled at 10,300-11,000 ft TVD using crosslinked gel with encouraging results. Although reservoir quality varies in the basin, the Turner interval is more than 30 ft thick in the area of interest (AOI) in Campbell County, Wyoming. In this area, production history matched permeability ranges from 0.005 to 0.1 mD, with pore pressure gradient from 0.55 to 0.64 psi/ft. Fracture modeling and production history matching/sensitivities were performed on a few horizontal wells. This paper discusses the results of this modeling and history matching, and it summarizes the evolution of Turner Formation fracture treatment designs, that were done by one operator to maximize the return on investment.

The operator collected core data, open hole logs, and Diagnostic Fracture Injection Test (DFIT) data. The objectives of this study were to: a) determine reservoir parameters from DFIT, b) estimate fracture height growth, fracture half-length, and conductivity for Turner crosslinked gel fracs, c) determine the most appropriate perforation cluster or fracture spacing, as well as treatment rate, fluid/proppant loading, and proppant types/sizes based on the expected long-term production performance, d) compare the estimated production of cemented sleeve vs. plug-and-perf completions, and e) perform multivariate analysis of public production and completion data to compare with the detailed physical modeling.

The results presented in this paper show well-performance predictions as a function of sleeve/perforation cluster spacing, treatment size, proppant type, mesh size, and pump rate. Implications for implementation of a certain treatment and completion design are discussed in detail.

Introduction

The Turner Sandy Member of the Carlile shale is geographically located in Northeast Wyoming. This low permeability oil sandstone interval overlies the Greenhorn and underlies the Niobrara Formation. The Turner reservoir on the east flank of the PRB (henceforth referred to as "basin") is the time equivalent of the

Frontier or Wall Creek interval on the western flank of the basin. The source rocks for the Turner reservoir are believed to be the underlying Mowry Shale and overlying Upper Cretaceous shales (Dolton and Fox, 1996). Ruhle and Orth (2015) reviewed production trends within the basin. They showed that gas-oil ratios (GORs) range from 600 to 3,000 scf/bbl with an average oil gravity of 43° API for Turner wells. They also reported that a variation of crosslinked and hybrid fluids has been pumped for Turner wells, with hybrid fluids showing higher production. The study showed that the wells treated with resin-coated proppant outperformed the wells treated with sand only and that, although slickwater wells (only two wells) performed more poorly than the crosslinked and hybrid wells, the result was not statistically significant.

Ingle, T. et al. (2017) investigated cluster effectiveness on the Parkman horizontal wells using Distributed Temperature Sensing (DTS) and Distributed Acoustic Sensing (DAS). They found that only 50% of the entry points in a stage were effectively stimulated. Gonzales, D. et al. (2017) highlighted the importance of a proper reservoir fluid characterization when developing a reservoir simulation model for an Upper Cretaceous tight sand field in the basin near the town of Douglas in Converse County, Wyoming. Three different reservoir fluid phases were identified in this study: black oil, volatile oil, and gas condensate fluid systems. Olaoye, O. et al. (2016) studied production drivers of Turner horizontal wells in the fringe of the play. They noted that there is no significant difference in productive fracture half-length for the plug-and-perf (PnP) vs. sliding sleeve treatments.

The purpose of this paper is to review the evolution of completion practices, evaluate the results of different completion design trials on several Turner horizontal wells, and identify areas for improvements. The existing literature suggests that while the basin contains one of the largest oil and gas resources in the U.S., historical information about how completion designs in the study area have evolved with time is lacking. Knowledge of prior completion practices could allow the operator to increase the profitability of horizontal well development in the basin. As of Q3 2018, more than 370 horizontal wells have been completed in the Turner Formation, of which 145 are in the operator's AOI, T42-43N and R72-74W. Several challenges of producing the low permeability oil sandstone (Turner) reservoir economically include, but are not limited to:

1. Reservoir fluid characterization and PVT analysis (uncertainty in the reservoir pressure and bubble point pressure variations across the basin).
2. Production induced pressure depletion, from both previously active vertical wells and existing horizontal wells, which could affect completion design programs and lead to premature GOR increases later in the life of the well.
3. Out-of-zone fracture growth—Turner interval thickness is only 30-50 ft in the study area.
4. Proppant selection due to a high-stress environment
5. Benefit of improving high cluster efficiency in PnP completions through pin point fracs.

Study Area

The K-Bar Field was discovered in 1976 according to The Wyoming Oil and Gas Conservation Commission or (WOGCC) and it is situated in the east-central part of the basin covering areas within the T42-43N and R72-74W in Campbell County, Wyoming. The field extends approximately 15 miles (northwest to southeast) by 12 miles (west to east). Fig. 1 shows a map of oil and gas production from horizontal Turner wells. While the basin comprises of many hydrocarbon productive intervals, the focus of this paper is the Turner Sandy Member interval. In the K-Bar Field, this reservoir has oil gravities from 40° to 44° API and a bottomhole temperature of 250°F, and it is historically over-pressured with pore pressure gradients as high as 0.64 psi/ft. In other areas outside of this operator acreage, the Turner horizontal wells that are actively developed by other operators may be under-pressured such as those on the fringe of the play in Niobrara County. The fluid properties in the Turner Formation are not uniform and the GOR tends to increase from northwest to southeast in the AOI.

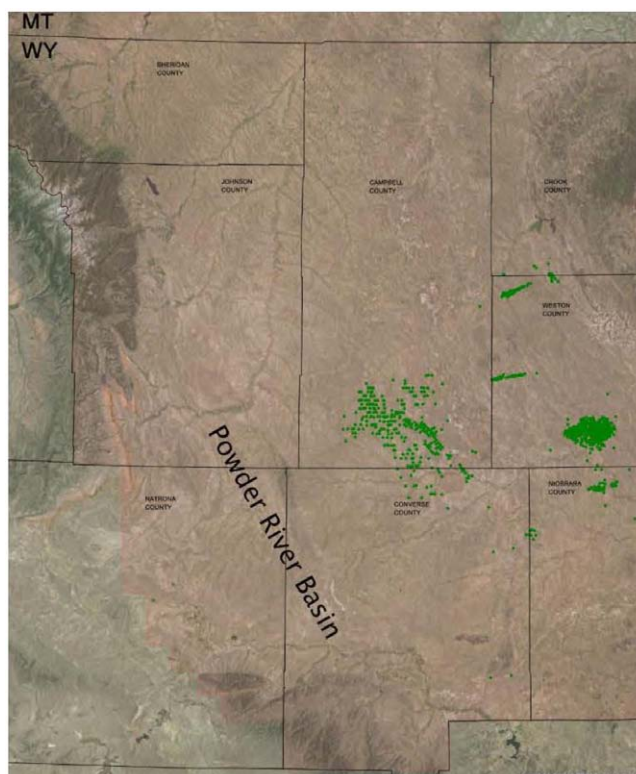


Figure 1—Map of the Powder River Basin showing oil and gas production of Turner Sandy Member of the Carlile Shale. The operator's AOI is in south-central Campbell County, where the Turner interval is found at 10,600-10,700 ft TVD as compared to that in Niobrara County, where the Turner reservoir is encountered at shallower depths of 4,000-5,000 ft TVD.

The operator collected core data and logs on several wells. The core data and full-suite triple or quad combo logs were available. The LT 21-7TH (see Abbreviations section) was cored and the side core samples collected were analyzed. These core samples showed that porosity ranges from 4.6 to 10.2%, and permeability varies from 0.0004 to 0.06 mD (Fig. 2). Fig. 3 shows geomechanical parameters on the vertical pilot hole (LT 14-2TH). The closure pressure stress differential is 600 psi lower in the Turner than the overlying Sage Breaks and 800 psi lower in the Turner than the underlying Greenhorn.

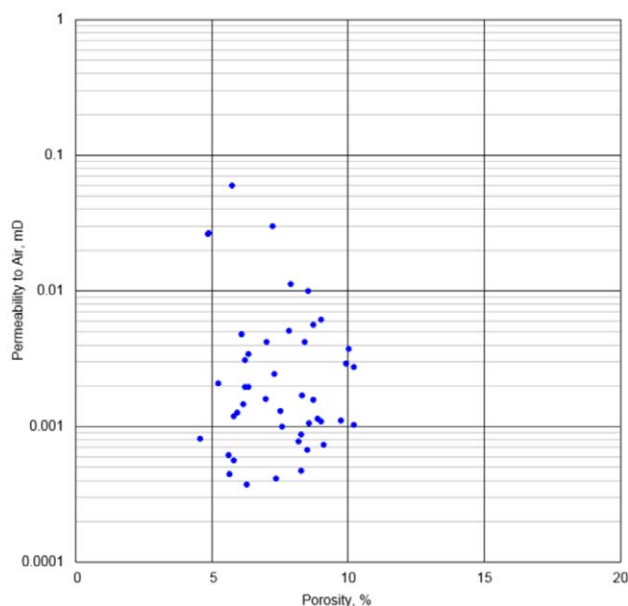


Figure 2—Core permeability vs. porosity crossplot for the Turner Sandy Member in the AOI.

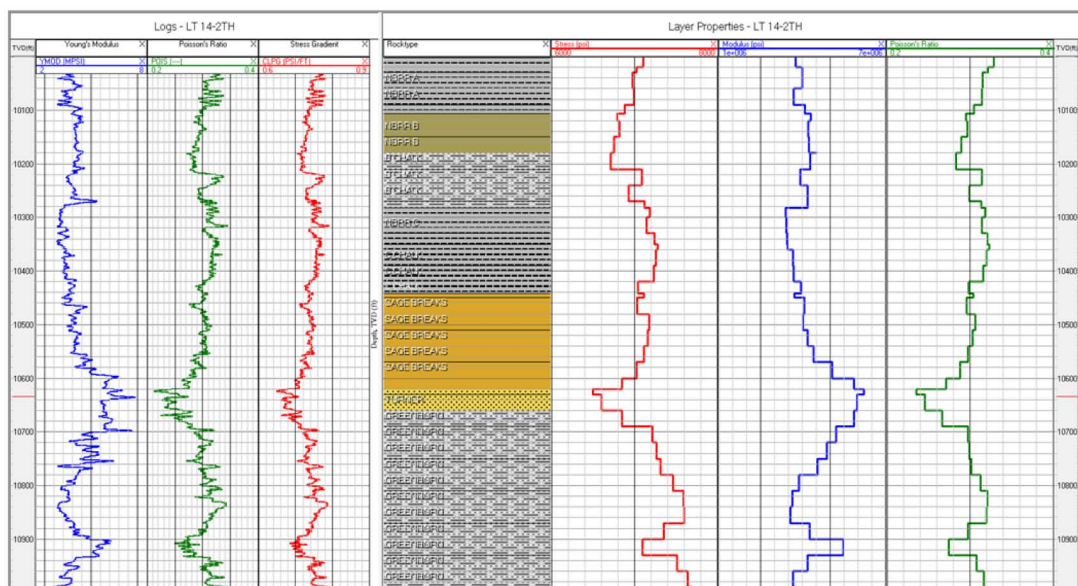


Figure 3—Geomechanical parameters: Young's Modulus, Poisson's Ratio, and minimum horizontal stress on the vertical pilot hole LT 14-2TH.

Completion Design History

The first Turner horizontal well, the Drake Federal 31-29TH, was completed by this operator in February 2012. The initial fracture design pumped on this well relied on early experience with Turner vertical wells and past completion practices in the basin. The early treatments pumped in 2012 laterals (~3,000 ft long) included 16 stages using 200 klb of 16/30 Interprop (intermediate-strength bauxite proppant) and 2,035 bbl of 25# crosslinked gel fluid per stage with 13 bbl of 7.5% acid per stage at 34 bpm treatment rates. These treatments were completed using a PnP completion with typically three to four clusters per stage, 0.42" EHD, 6 spf, 60° phasing, and 1.5" guns. The use of crosslinked gel in these jobs has some advantages. The gel provides sufficient viscosity for proppant transport and ensures that the fracture propagates deeper into the relatively high permeability matrix. Unlike slickwater fluid where the high velocity of the injected water is the transporting mechanism, the crosslinked gel system transports proppant through high viscosity with minimal leakoff ([Al-Muntasheri, 2014](#)). This early design has been modified over time after evaluating the post-treatment well performance. For the subsequent completions, the proppant types pumped have included sand and ceramic as well as pre-cured and cured resin coated sands (PRC and CRC were mainly used as tail-ins).

The operator completed several more Turner horizontal wells using PnP and sleeve completions in 2013. The treatments consisted of 17 stages with a maximum proppant concentration of 4 ppg and 16/30 ISP ceramic at 26 to 30 bpm. The operator later experimented with more stages (e.g., 21 stages using a combination of sleeves and PnP on the same lateral), 200 klb of 20/40 PRC sand, and 33% more fluid per stage (2,706 bbl of 25# crosslinked gel). In this "optimized" design, the sleeves were spaced 170 to 180 ft apart at the toe of the lateral followed, by low rate (30 bpm) PnP stages that had two clusters spaced at 84 ft apart. The use of a PRC tail-in is meant to increase the proppant crush resistance as pressure drawdown occurs. The PRC helps to reduce embedment and fines migration in the fracture, but, it is not intended to prevent proppant flowback, which was not a concern in these wells.

The Turner horizontal wells completed by this operator in 2014 utilized only pin point fracs (sleeves) from 17 to 21 stages with 200 klb of 20/40 PRC sand and about 2,200 bbl of 25# crosslinked gel per stage. The average pump rate was low (~30 bpm). In 2015, the operator increased the lateral length to 3,500 ft and the number of stages to 32 using sliding sleeves at varying spacings from 85 to 145 ft. This design resulted in a significant production improvement due to more stages and longer laterals. To date, one of the wells

that utilized this design (D44-15TH) is still one of the best wells completed in the AOI. The operator shifted focus in 2016 and 2017 to focus on horizontal Parkman development, but resumed Turner drilling in 2018. Slickwater-only design (often used in very low-permeability reservoirs where leakoff is very small) has not been used by this operator to complete Turner horizontal wells.

While the vast majority of the operator's completions were PnP, operationally, the operator has successfully completed more than 120 sliding sleeves on 7 horizontal wells in the basin without a single screenout. The operator has also used a mix of treated and fresh water with 4% KCl in completion program to increase profitability of its assets.

Statistical "Big Picture" Analysis of Public Production and Completion Data

A production and completion database was populated using various sources including the WOGCC and using commercially available data. There were 27 Turner horizontal wells completed by this operator with more than 365 producing days. The well count increased to 129 when other operators were considered. Qualitative analyses of the 365-day cumulative oil production data, normalized to feet of lateral length for these 129 wells, reveal a positive correlation between the normalized 365-day cumulative oil production data and proppant mass and a weak negative correlation between the normalized 365-day cumulative oil production data and % Sand, indicating that premium proppants (ISP and RCP) could result in slightly better production (Fig. 4). The diminishing production benefit of larger proppant loadings appears to occur around 1,200 lb/ft. There was not enough variability in the size of proppants used to establish a correlation because many wells did not have a reported proppant size and of those that did, almost all used a similar combination of 20/40 and 40/70 proppant.

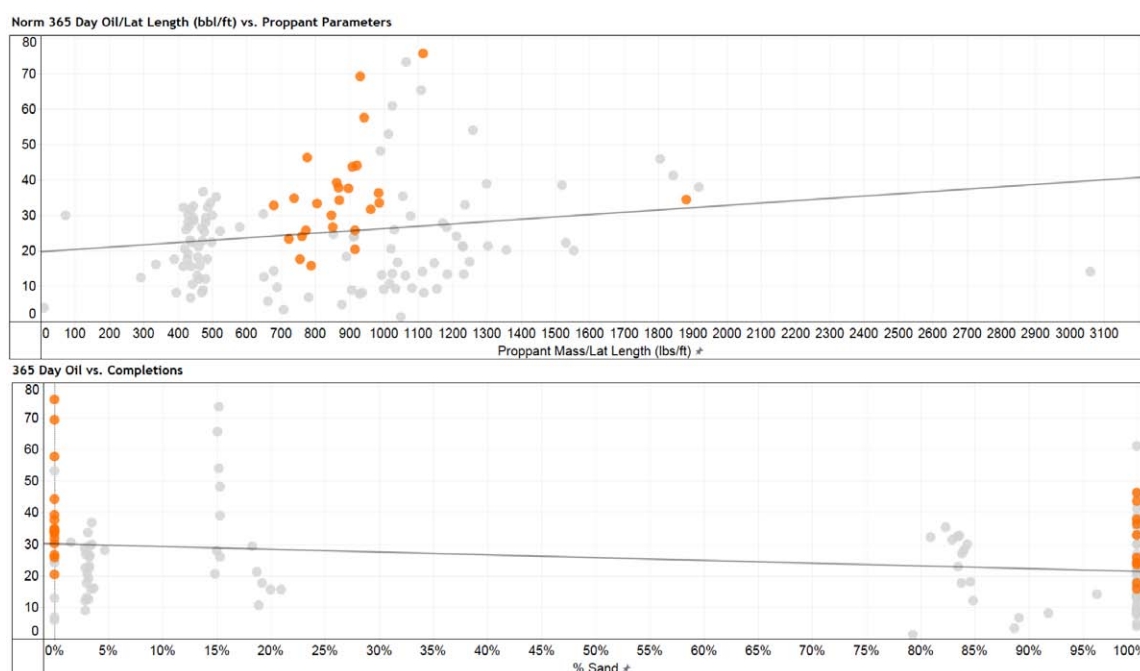


Figure 4—Bivariate plots showing weak correlations between the normalized 365-day cumulative oil production data and proppant mass per lateral foot as well as percentage of sand pumped. Orange data points are wells belonging to the operator of interest and grey are other operators in the study area.

There is an indication of negative relationship between normalized 365-day cumulative oil production and 365-day water cut as well as stage length: as stage length increases, oil production decreases. Total clean volume of fluid/lateral length (bbl/ft) has a positive relationship with normalized production, indicating that overall job size has some positive correlation with production. Diminishing returns on fluid volume can be

seen around 15 bbl/ft. There is a weak negative correlation with average PPG, indicating a relative increase in fluid volume without a corresponding increase in proppant volume could positively impact normalized 365-day cumulative oil production (Fig. 5).

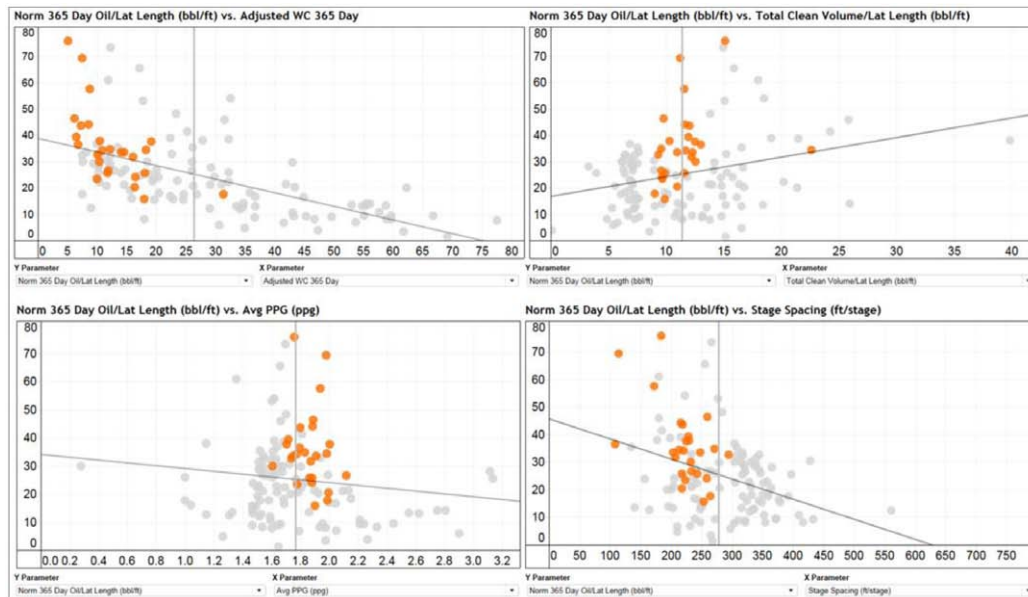


Figure 5—Bivariate plots of normalized 365-day cumulative oil production/ft vs. water cut, total clean volume pumped/ft, average PPG, and stage spacing showing weak correlations. Orange data points are wells belonging to the operator of interest and grey are other operators in the study area.

DFIT Analysis

Several Turner DFITs were pumped by this operator in the operator's AOI. These tests provide valuable information such as fracture gradient, closure pressure, pore pressure, and reservoir permeability. These parameters are critical inputs for fracture and reservoir models. The results show an average fracture gradient of 0.71 psi/ft and an average closure pressure gradient of 0.62 psi/ft. The average pore pressure gradient is 0.59 psi/ft. The reservoir permeability estimates from DFITs range from 0.05 to 0.6 mD, but these estimates should be considered an upper limit because the data is gathered under injection conditions. The core permeabilities are shown in Fig. 2. Table 1 summarizes the DFIT analysis results for the Turner Sandy Member interval in the study area.

Table 1—DFIT analysis results summary in the Turner Sandy Member interval.

DFIT	Well	BH ISIP (psi)	Closure Pres. (psi)	Pore Pres. (psi)	FG (psi/ft)	Closure Pres. Grad. (psi/ft)	Pore Pres. Grad. (psi/ft)	Reservoir Perm (mD)
1	D24-30TH	7,159	6,894	6,726	0.68	0.66	0.64	0.05
2	D41-24TH	7,740	6,390	6,004*	0.73	0.60	<0.57	0.16
3	D44-15TH	7,367	7,004	6,621	0.68	0.65	0.62	0.08
4	LT41-34TH	7,557	6,632	6,173	0.71	0.62	0.58	0.60
5	R42-5TH	8,055	6,696	6,032	0.73	0.61	0.55	0.28
6	R44-24-1XTH	7,716	6,631	5,950	0.71	0.61	0.55	0.05

*Upper bound

Fig. 6a (left) shows a G-function plot on the D44-15TH where closure pressure is estimated at 7,004 psi (0.65 psi/ft) with a closure time of 57 hours. During the DFIT, the net pressure was observed to be 363 psi with a fluid efficiency of 94%. The leakoff behavior appears to be dominated by the matrix with a minor pressure dependent and fracture height recession leakoff during the shut-in. Fig. 6b (right) shows the G-

function plot on the D41-24TH. The semilog derivative shows a pressure dependent leakoff signature due to dilated fractures/fissures—as indicated by a characteristic hump in the superposition derivative that lies above an extrapolated straight line through the normal leakoff data. The DFIT performed on the D41-24TH shows a closure pressure of 6,390 psi (0.60 psi/ft) and a closure time of 10.5 days. This long closure time was due to injecting a large volume of DFIT (approximately 2,750 bbls) at 30 bpm—because there was no clear indication that the sleeve had shifted. This was done to ensure that the target rate would be achieved prior to rigging up an entire frac fleet (Fig. 7). Hence, there was some uncertainty with the large volume of water pumped to ensure that sleeves were shifted open. There also was a learning curve with pumping initial DFITs in the study area. A certain degree of communication with offset wells during the DFITs was also observed. In the basin, an additional challenge exists in the winter where the gauges stopped collecting data due to being frozen (we pumped heavy brine fluid to mitigate this problem).

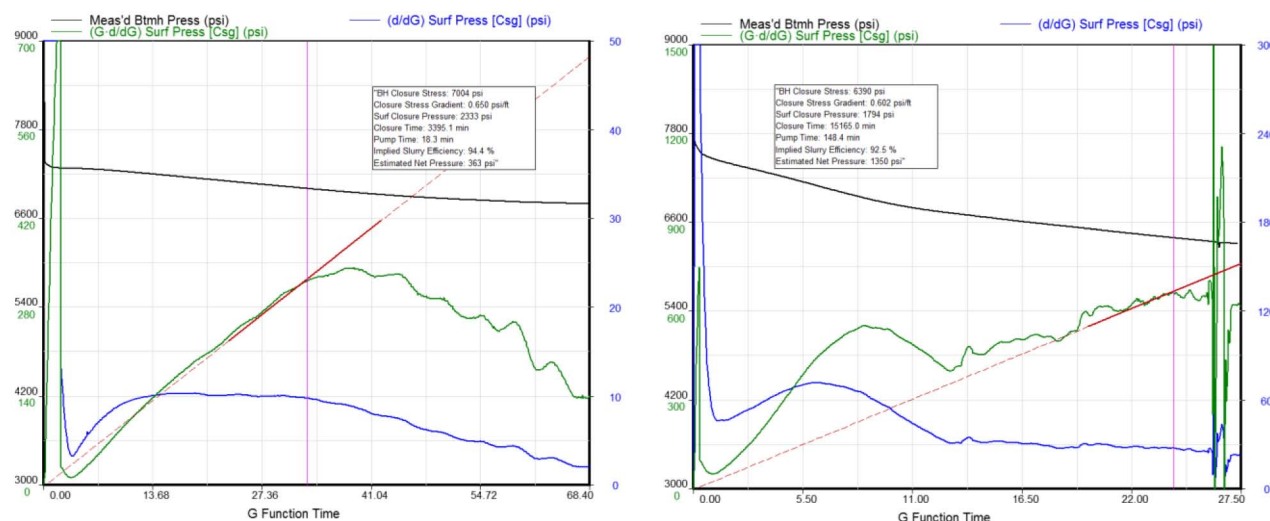


Figure 6—G-function plot on the (a) D44-15TH DFIT indicating a minor pressure dependent and fracture height recession leakoff, and (b) D41-24TH DFIT indicating a significant pressure dependent leakoff.

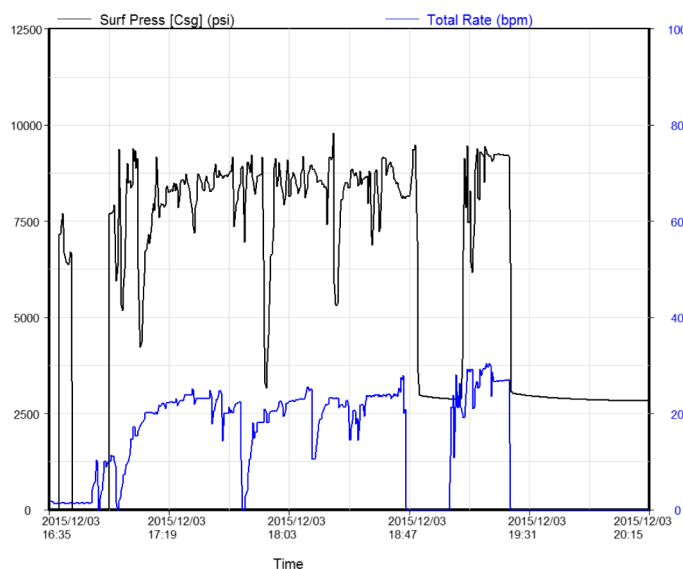


Figure 7—Long injection period and shut-in sequence on the D41-24TH DFIT.

Fracture Modeling

Fracture modeling was performed with the goal of matching the observed fracturing net pressure (fracturing pressure minus minimum rock stress or closure pressure) and determining fracture dimensions and conductivity. A 3D lumped fracture model was used in this study. Fig. 8 shows a good match of modeled net pressure (red) vs. observed net pressure (black) for a sleeve stage on the D44-15TH. This stage used 105 klb of 20/40 RCP sand and 1,200 bbl of 25# crosslinked gel pumped at 15 bpm. The lateral was completed with a proppant loading of approximately 970 lb/ft and the frac gradient was 0.81 psi/ft. The pressure match resulted in a propped fracture half-length of 550 ft and a propped height of about 130 ft. These results were subsequently used to build the reservoir model described in more detail later. Although no microseismic mapping (MSM) was performed by the operator during Turner completions, the MSM data on the GDU44-8PH well (Parkman) reveals that out-of-zone height growth may occur due to lack of sufficient stress barriers at adjacent layers. Fig. 9 does show some but not excessive out-of-zone height growth for the above sleeve stage treatment.

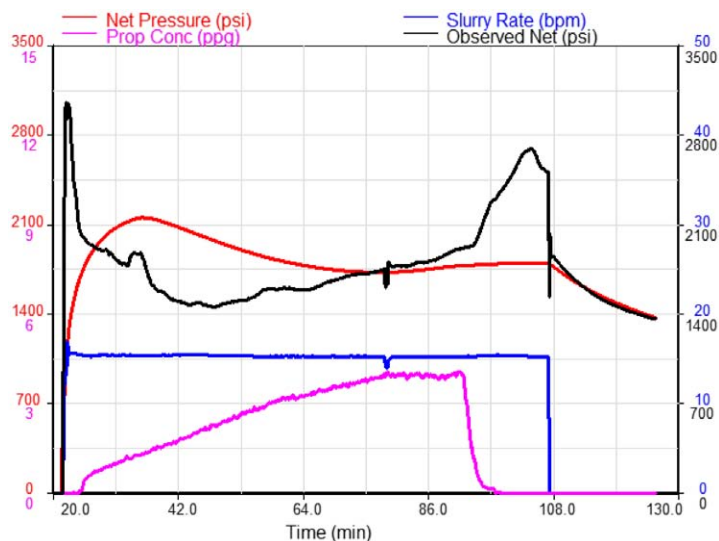


Figure 8—Net pressure match of a sleeve stage pumped on the D44-15TH showing a good match between the modeled and observed net pressures during pump shut-down.

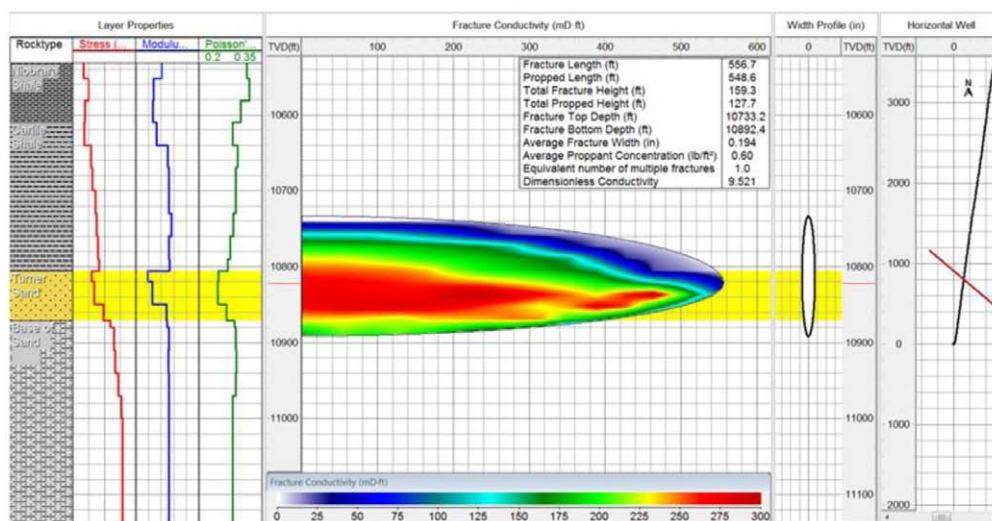


Figure 9—Fracture geometry for a sleeve stage pumped on the D44-15TH showing an out-of-zone height growth above and below the Turner Sandy Member interval.

Table 2 shows a summary of well completion designs and fracture modeling results on two selected Turner wells completed in 2015. As shown, the PnP jobs resulted in shorter fracture lengths than the sleeve jobs. In case of D24-30TH, the treatment size is double for the two-perforation cluster PnP stage versus the sleeve stage, but the pump rate of 30 bpm is split into two perforation clusters, which may not be as efficient for length generation as the higher rates into a single sleeve. In case of LT 41-34TH, the fluid and proppant volumes on a per cluster basis for the PnP stage are half of what is pumped for the sleeve stage, thus the fracture half-length is about 30% shorter. The sleeve completions intend to generate at least one fracture per stage while with PnP, the goal is to have better control over the location and higher number of entry points along the wellbore with less stages required. For PnP completions, the exact fluid and proppant volumes that enter each cluster are unknown without other advanced diagnostics (Ingle, T. et al., 2017). Table 2 also summarizes end-of-job slurry efficiency. The slurry efficiencies are fairly low indicating higher leakoff compared to ultra-tight unconventional reservoirs.

Table 2—Comparison of standard sleeve and plug-and-perf completion designs with fracture modeling results.

	D24-30TH		LT 41-34TH	
Stage number	9	10	5	7
Completion type	Sleeve	Plug-and-Perf	Sleeve	Plug-and-Perf
Total clean fluid pumped, bbl	1,319	2,437	2,441	2,312
Total proppant pumped, lb	95,800	198,900	199,100	200,200
Proppant size and type	20/40 PRC	20/40 PRC	20/40 PRC	20/40 PRC
Frac fluid system	25# XL	25# XL	25# XL	25# XL
Average pump rate, bpm	30	30	30	31
Max. proppant conc., ppa	4.0	3.8	4.0	4.1
Number of fractures per stage	1	2	1	2
Fracture half-length, ft	475	425	613	423
Fracture height, ft	93	102	241	135
Average fracture cond., mD-ft	345	303	345	410
Surface ISIP, psi	3,886	3,476	3,776	4,096
Fracture gradient, psi/ft	0.80	0.76	0.79	0.82
Observed net pressure, psi	1,548	1,141	1,756	2,077
EOJ slurry efficiency, %	36	35	30	16

Production History Matching and Sensitivities

Post-treatment production data on the D44-15TH was history matched to calibrate reservoir model parameters. The resulting calibrated numerical model could then be used for sensitivity analysis to determine the optimal cluster or fracture spacing, treatment rate, fluid/proppant loading, and proppant types or sizes. The subject horizontal well was drilled along a N8°E azimuth at a depth of approximately 10,800 ft in the Turner interval. A three-phase blackoil reservoir model was set up using a commercial reservoir simulator. The gridded model simulates a 5,280 ft by 5,280 ft drainage area, a single horizontal well, and a single reservoir layer representing the Turner Formation. Since there were no "competing" adjacent laterals during the production history match period, an infinitely acting reservoir was simulated by placing no-flow boundaries far enough from the wellbore. The lateral length was 3,700 ft with 32 stages using a sleeve completion with a variable sleeve spacing. The plan view of the reservoir model is shown in Fig. 10.

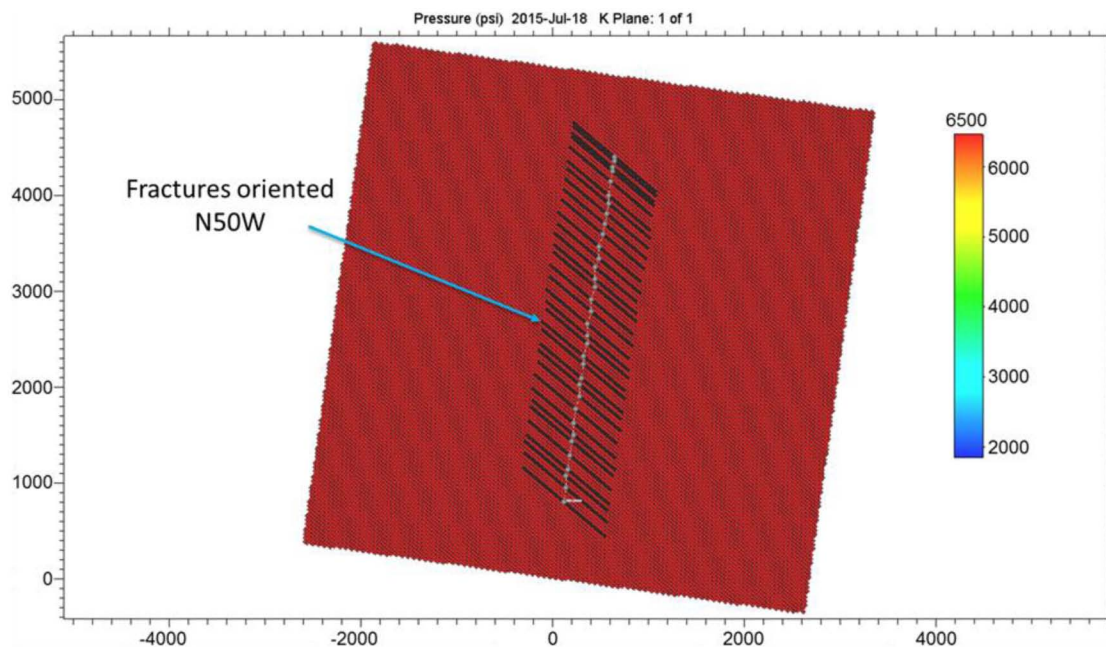


Figure 10—Reservoir model setup showing the gridded hydraulic fractures and colored by initial reservoir pressures.

The DFIT reservoir permeability of 0.08 mD and pore pressure of 6,500 psi were used as initial input for the reservoir model. In the automated history matching process, the reservoir permeability ended up being reduced to 0.009 mD, which is a common downward adjustment since DFIT permeabilities are typically an upper bound. Other layer properties such as porosity and water saturation were based on petrophysical analysis. Basic hydrocarbon properties such as oil and gas gravities were obtained from PVT analysis reports from nearby wells. The rest of the PVT data was generated using standard correlations in the reservoir simulation software. The bubble point pressure was varied during the history matching process to match the observed gas-oil ratios. The initial fracture half-length of 550 ft and conductivity of 210 mD-ft were based on the 3D lumped fracture modeling discussed in the previous section, but these parameters were also varied during the history matching. The fracture azimuth in the study area was assumed to be N50°W based on area stress data. Additional history match parameters were net-to-gross thickness, reservoir permeability, initial water saturation, and matrix relative-permeability curves. In this study, two sets of relative-permeability curves were used; one represents the matrix gridblocks and the other represents the fracture gridblocks. Straight-line relative permeability curves were assigned to the fracture gridblocks, while the Corey-type, power-law correlations were used to generate the matrix relative permeability curves. The power-law exponents and the relative permeability end-points were varied to match the observed production data.

The history matching process consisted of constraining the oil production rate to the observed oil rate and matching the model-predicted well-head pressures, gas rate, and water rate to the observed data simultaneously. Since measured bottom-hole pressures were not available, well-head pressures were calculated from the modeled bottom-hole pressures using a wellbore flow correlation (Petalas-Aziz mechanistic model). No artificial lift was installed during the early-time production period, but after six months of production, a 2-3/8" velocity string was installed in the wellbore. With regards to the observed water rate, the initial water production was affected by flowback water. Consequently, emphasis was placed on matching only the stabilized water production (after a few months of production).

A commercially available assisted history matching tool was utilized to history match the production data. This process involves setting up an optimization problem by defining an objective function to be minimized or maximized by varying specified parameters. For this history matching, the objective function to be minimized was the weighted average of the difference between the modeled and measured well-head

pressures, gas rate, and water rate. The history match parameters included the fracture half-length, fracture conductivity, number of fractures, net-to-gross thickness, reservoir permeability, initial water saturation, and matrix relative permeability curves. In our study, the optimizer explored approximately 500 solutions to arrive at the optimal solution (i.e., a solution with the lowest value of the objective function). Table 3 shows the parameters used in the final history-matched reservoir model.

Table 3—Parameters used in the history matched model

Parameters	Value
Net pay thickness, ft	88
Reservoir permeability, mD	0.009
Porosity, %	12
Reservoir pressure, psi	6,500
Oil gravity, °API	44
Gas gravity	1.42
Reservoir temperature, °F	248
Bubble point pressure, psi	3,700
Initial water saturation, fraction	0.375
Connate water saturation, fraction	0.3
Fracture conductivity, mD-ft	135
Fracture half-length, ft	550
Number of effective fractures	32

Fig. 11 shows the history match results. On the top-left is the observed oil rate used as a simulation constraint. The top-right plot shows the observed (blue) vs. predicted (red) well-head pressures and the bottom-left plot shows the observed vs. predicted gas rates, indicating very good matches. The bottom-right plot shows the observed vs. predicted water rates, indicating a good match in the late time (early time data was affected by fracturing fluid flowback and was not matched in this study).

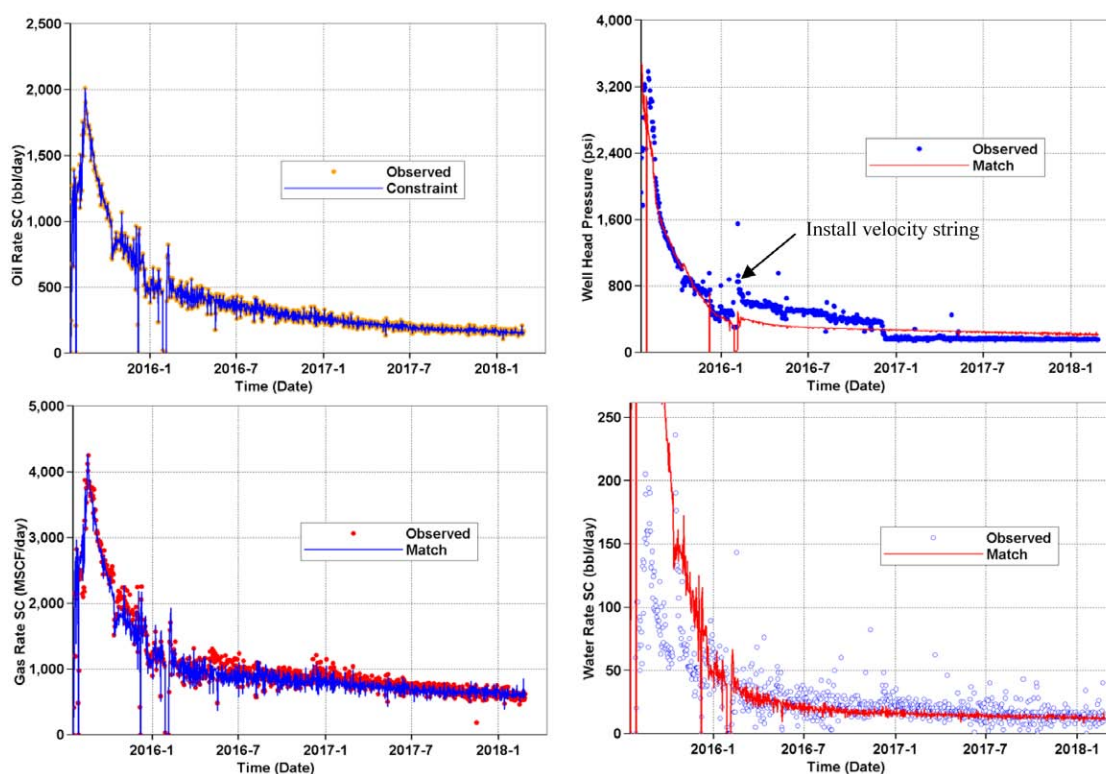


Figure 11—Observed oil rate as a simulation constraint (top left), model vs. observed well-head pressures (top right), model vs. observed gas rates (bottom left), model vs. observed water rates (bottom right).

After the history match was completed, the next step was to evaluate whether the completion design could be improved for the new adjacent lateral to be drilled at a well spacing of 1,550 ft from the existing lateral. Fig. 12 illustrates the pressure depletion at the end of the history match period (approximately 950 days) along with the approximate location of the new lateral 1,550 ft away from the history-matched lateral. Sensitivities were performed to determine the most appropriate fracture spacing, proppant loading, pump rate, and proppant type in this new lateral. Since the new well was yet to be drilled in an almost virgin reservoir, the sensitivities were performed on a single well model with no-flow boundaries placed at 775 ft or half the well spacing on either side of the lateral.

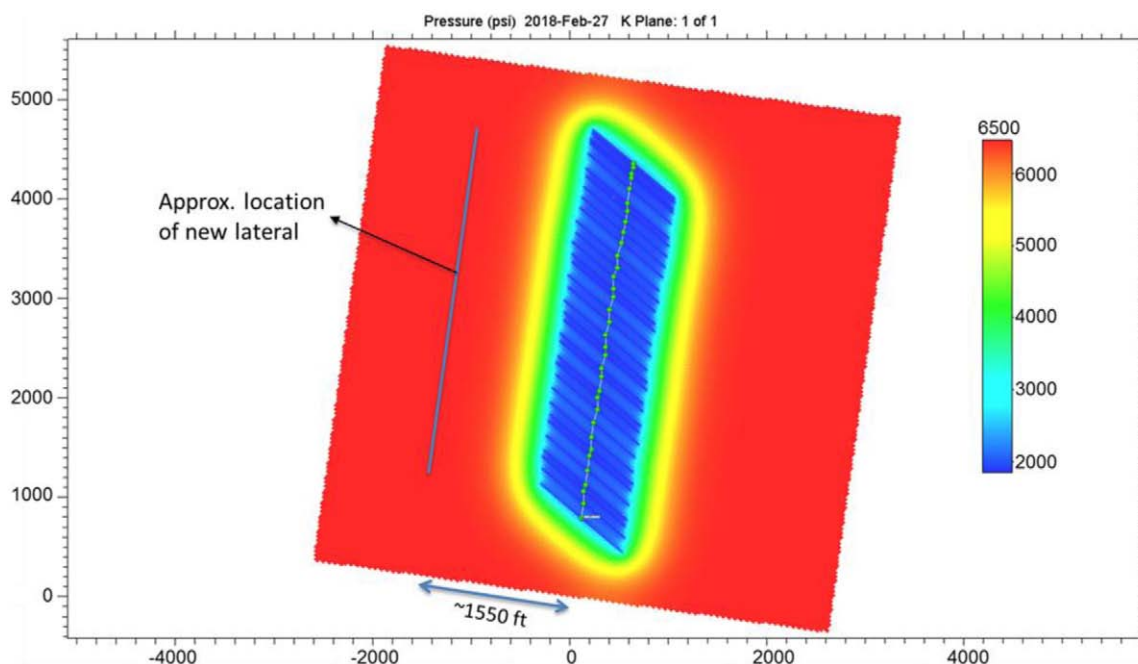


Figure 12—Pressure profile at the end of the history-match period and approximate location of the new lateral.

Production sensitivity to fracture spacing was performed assuming the proppant loading per feet of lateral length is constant. The base case fracture design was 970 lb/ft. A tighter fracture spacing would imply more fractures along the lateral. The total proppant volume, which was held constant, is distributed equally among these fractures (i.e., perforation clusters). This would result in smaller fracture geometries as the fracture spacing decreases. Note that fracture modeling was performed to determine the fracture geometry and conductivity at different fracture spacing scenarios. The fracture geometry and conductivity results for this fracture spacing sensitivity using a constant proppant loading of 970 lb/ft are shown in Fig. 13. These results were then used in the reservoir modeling. The reservoir model was run assuming a 500-psi minimum flowing bottom-hole pressure from the start of the simulation. As a result, the absolute production numbers would be somewhat optimistic. Therefore, the emphasis should be on the relative differences in the estimated well production due to different fracture-spacing scenarios.

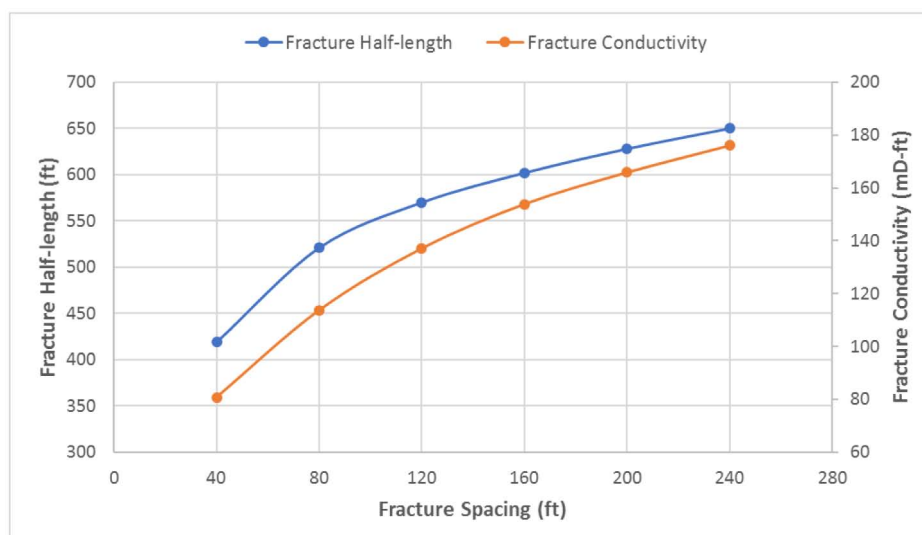


Figure 13—Fracture modeling results for fracture spacing sensitivity at constant proppant loading of 970 lb/ft.

The cumulative oil production response at different fracture spacings is shown in Fig. 14. Based on the one-year cumulative oil production, this simulation shows that there is no benefit to decreasing the fracture spacing below 120 ft. The production acceleration at lower fracture spacing scenarios (i.e., less than 120 ft) is more than offset by the decrease in fracture length and conductivity based on constant proppant loading. On the other hand, the long-term production (e.g., a 5-year cumulative oil production) increases with fracture spacing up to 200 ft. For example, at the end of the 5-year period, the scenario with a fracture spacing of 200 ft results in approximately 33,000 bbls of additional oil than the scenario with a fracture spacing of 120 ft. Again, Fig. 14 is valid when the proppant loading is kept constant at 970 lb/ft. The longer fracture half-lengths and larger fracture conductivities, generated at larger fracture spacings (in Fig. 14), contribute to the incremental production in the long run. The optimum fracture spacing will depend on the balance between maximum short-term and long-term production. For this area, a 120 ft fracture or cluster spacing appears optimal when maximizing the one-year (short-term) production, while still resulting in "acceptable" long-term production. Fig. 15 compares the pressure depletion at the end of 10 years for two different fracture spacing scenarios: 40 vs. 240 ft. The larger drainage area (due to longer fracture half-lengths and higher conductivities for the case of 240-ft fracture spacing) leads to higher cumulative oil production.

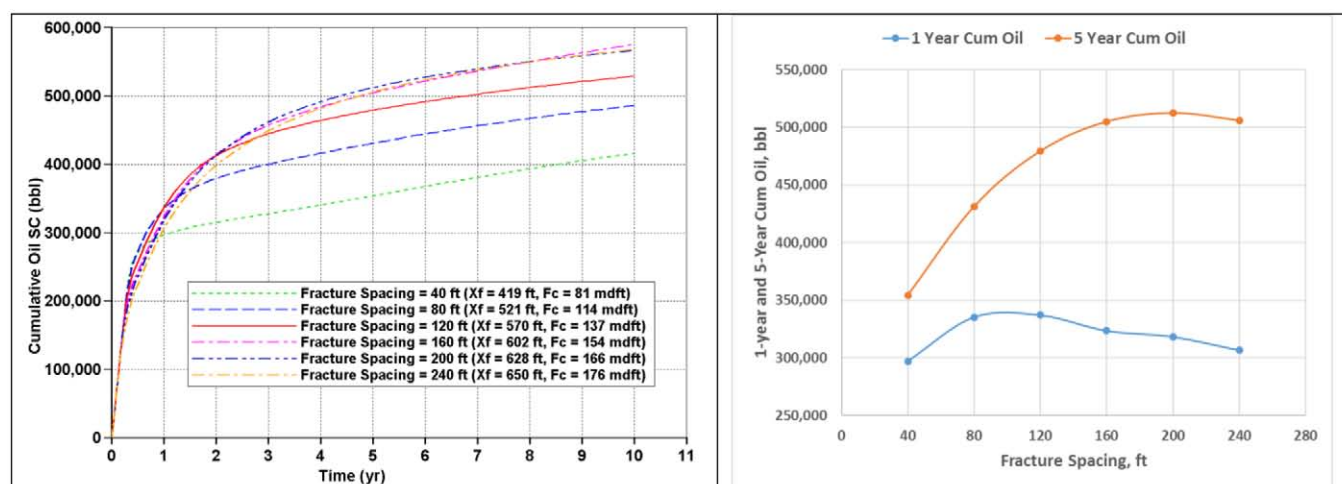


Figure 14—Cumulative oil sensitivity to fracture spacing at constant proppant loading of 970 lb/ft. Left: Cumulative oil vs time at various fracture spacings. Right: One and five-year cumulative oil vs. fracture spacing.

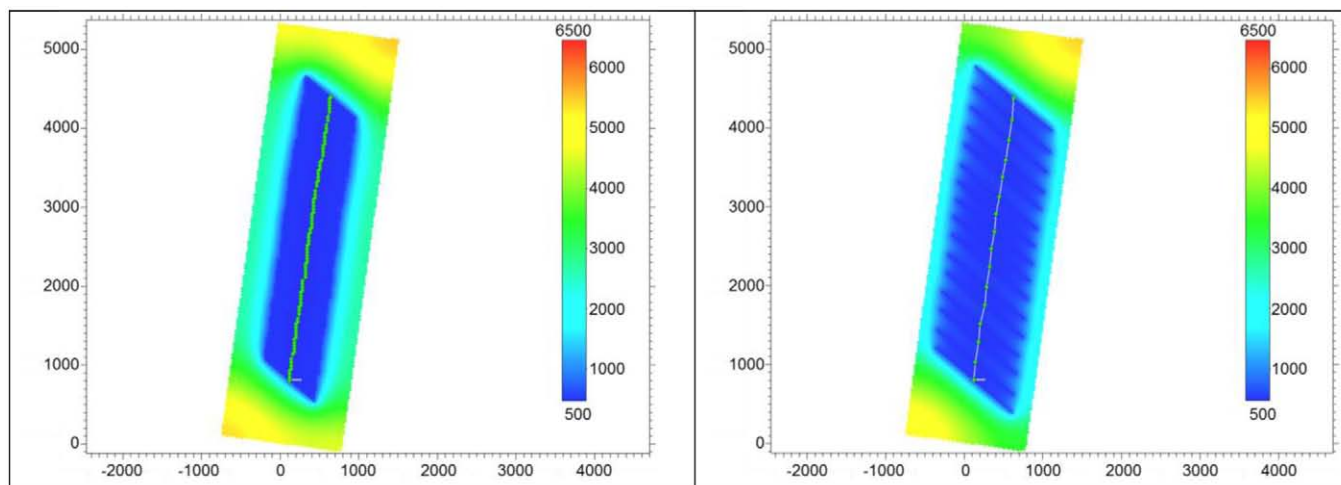


Figure 15—Comparison of the pressure depletion after 10 years for fracture spacings of 40 ft (on left) and 240 ft (on right).

After finding the optimal fracture spacing for a given proppant loading of 970 lb/ft (e.g., 120 ft), the next step involved performing sensitivities to proppant loading, that is, the total proppant mass pumped per well divided by the completed lateral length. As before, fracture modeling was performed to determine the fracture geometry as a function of proppant loading. The results are shown in Fig. 16, where increasing the proppant loading would appear to yield an increase in the fracture half-length and conductivity with diminishing changes for larger proppant loadings. Fig. 17 (left) shows the cumulative oil production vs. time for varying proppant loadings assuming a constant fracture spacing of 120 ft. Fig. 17 (right) shows a diminishing increase in both the one-year (short-term) and long-term cumulative oil production. Increasing the proppant loading from 970 to 2,000 lb/ft results in an additional 40,000 bbls of oil in one year and 48,000 bbls of oil in five years. Furthermore, there is only a slight incremental gain in oil production between 1,800 and 2,000 lb/ft of proppant loading. The benefit of higher proppant loading beyond 2,000 lb/ft appears to be very small. Additionally, the fracture lengths for very large proppant loadings would start to approach the planned well spacing in this area. In summary, the economic benefits of increasing the proppant loading from the current design (970 lb/ft) to 1,800 lb/ft look very attractive, but, would need to be evaluated in detail.

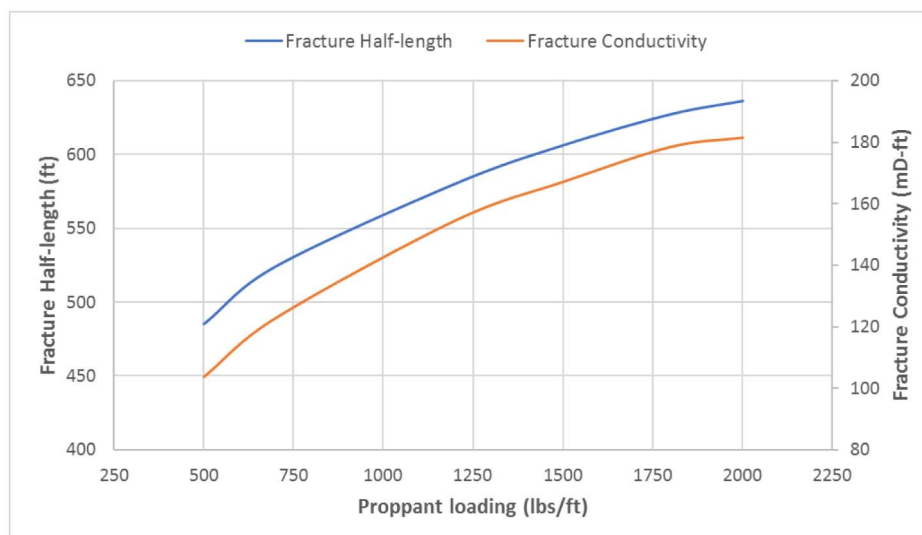


Figure 16—Fracture half-length and conductivity as a function of proppant loading.

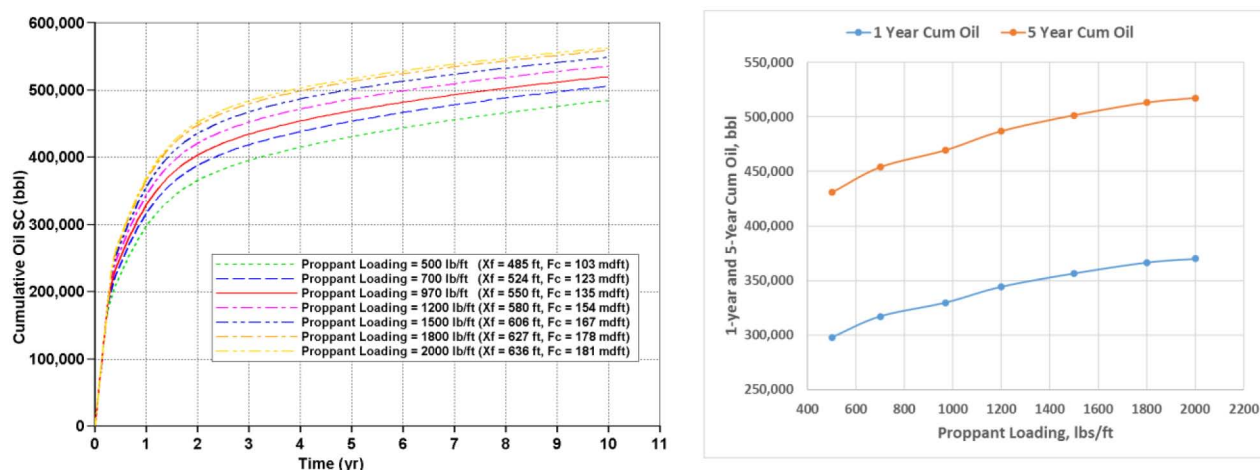


Figure 17—Cumulative oil sensitivity to proppant loading at a fracture spacing of 120 ft. Left: Cumulative oil vs time at various proppant loadings. Right: One- and five-year cumulative oil vs. proppant loading.

The next sensitivity performed was to pump rate. For a PnP completion, achieving a sufficient pump rate is critical for limited entry and effective stimulation of all clusters. However, even if a 100% cluster efficiency is assumed, pump rate can affect the created fracture geometry. This operator employed a PnP completion with two clusters per stage spaced 120 ft apart. Fig. 18 shows the fracture modeling results for 2 different proppant loading scenarios and sensitivity to pump rate. The chart shows that there is no significant benefit in terms of fracture length at pump rates of 40 bpm or higher.

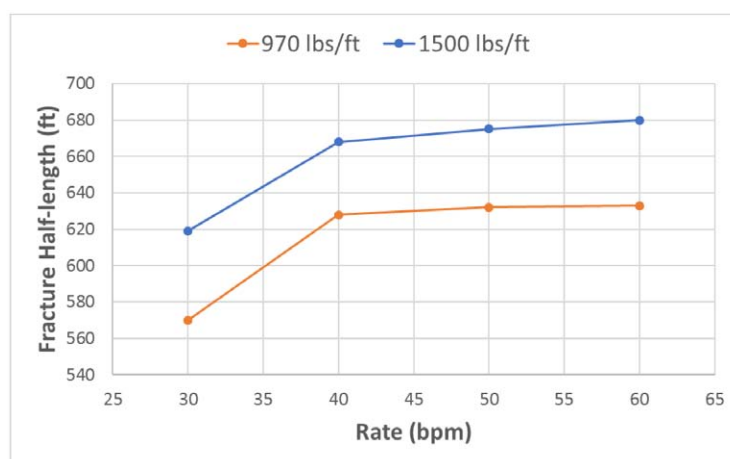


Figure 18—Propped fracture half-length as a function of pump rate for a plug-and-perf stage using two clusters.

The impact of using different proppant types was also evaluated. The current completion design used 20/40 PRC sand. A sensitivity looking at the potential production impact of switching to either a 20/40 ceramic or a 30/50 ceramic proppant was evaluated. In this sensitivity, fracture modeling that assumed the current proppant loading of 970 lb/ft indicated some changes in fracture conductivity with insignificant changes to the fracture geometry. The history-matched fracture conductivity using the 20/40 PRC was 135 mD-ft (see Table 3). In comparison, the frac model shows a fracture conductivity of 206 mD-ft using a 20/40 ceramic proppant and a fracture conductivity of 119 mD-ft using 30/50 ceramic proppant. Using these conductivity values, the reservoir model showed similar cumulative oil production estimates for all three cases (Fig. 19). This is not surprising because the fracture conductivities are relatively high, while the reservoir permeability is still relatively low (0.009 mD). This provides a dimensionless fracture conductivity greater than 20, which means that the fractures are essentially infinite conductivity.

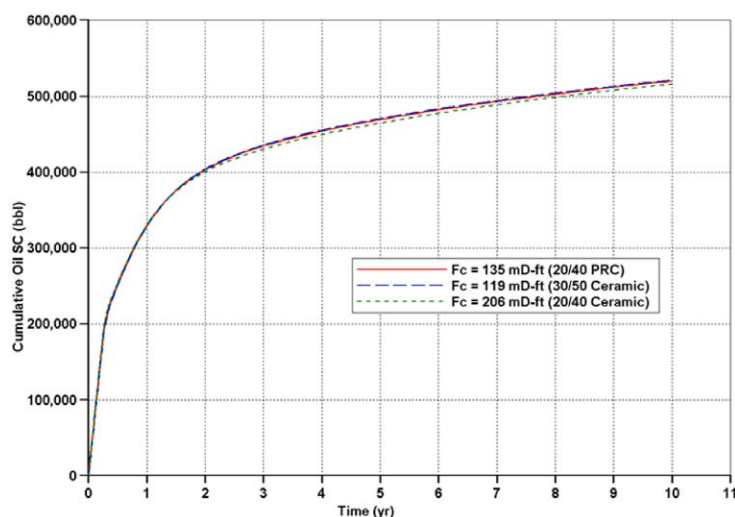


Figure 19—Cumulative oil production for different proppant types/sizes.

It is important to note that the reservoir permeability of 0.009 mD is still relatively higher than the permeability of many unconventional shale formations, but it is lower than the permeability of a typical conventional reservoir. Therefore, the design philosophy of the operator has been to employ crosslinked gel fluids to generate higher conductivity fractures. At the same time, the operational cost savings such as lower water volumes and pump rates as compared to those used in slickwater jobs also justify the use of the crosslinked gel system for this operator.

Multivariate Analysis

The previous sections describe the detailed fracture and reservoir modeling on a single well. A statistical analysis of multiple wells in the area can provide insight into the general trends and important factors contributing to the production response. A database containing information on approximately 40 variables and 347 horizontal wells completed in the Turner was analyzed. For this study, the response variable of interest is the 365-day cumulative oil production normalized by lateral length. Of the 40 variables, only eighteen were considered as potential predictors for building the multivariate statistical model. The other variables were excluded due to either missing values or multi-collinearity with the other predictors. The Alternating Conditional Expectations (ACE) approach was used to analyze the data similar to the work of [Lolon et al. \(2018\)](#). A backward selection was used to determine the final predictors. Eight of the potential 18 predictors were observed to be significant. After accounting for missing predictor values, the well count dropped to 257 wells. In addition, twelve wells were determined to be outliers, thus bringing the final well count for analysis to 245. The ACE model suggests optimal nonlinear transformations for both the response variable and predictors to maximize the linear correlation between the response and predictor variables. Closed functional forms for the ACE-suggested transformations were determined using linear spline or power-law functions. [Fig. 20](#) compares the predicted vs. observed 365-day cumulative oil production (bbl/ft). The R-squared value from this model is 0.80 with training and test RMSEs of 5.55 bbl/ft and 5.96 bbl/ft (26.4% and 28.4% of the mean, respectively). [Fig. 21](#) shows the predicted 365-day cumulative oil production (bbl/ft) vs. each predictor variable using the ACE model, while holding all the other predictors fixed at their mean values. These results show evidence of nonlinear relationships between production and reservoir and completion variables. Note that the production response with respect to proppant mass shows a slope change at approximately 1,250 lb/ft, with a more moderate slope beyond this point (less incremental oil production for a given additional lb/ft proppant mass). The decrease in slope above 1,250 lb/ft is purely data-driven and does not suggest that the optimum proppant mass for this area is 1,250 lb/ft. The optimum proppant mass would depend on the actual pad development scenarios and cost structures.

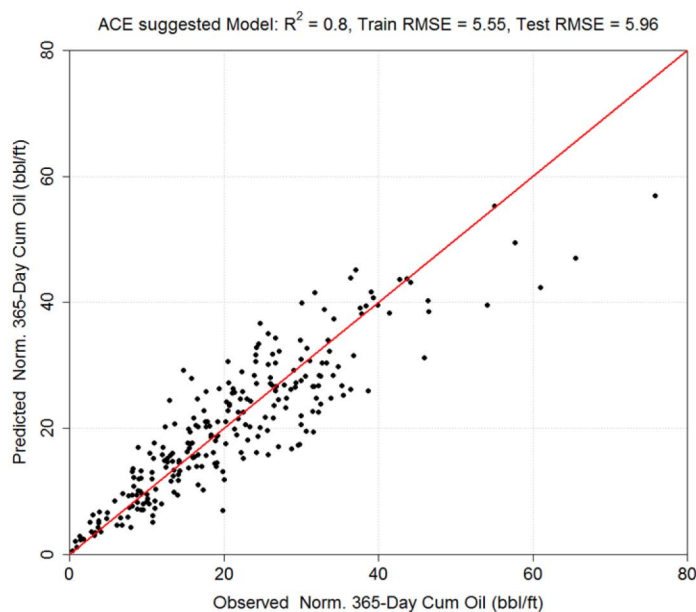


Figure 20—Predicted vs. observed 365-day cumulative oil production (bbl/ft) using the ACE algorithm.

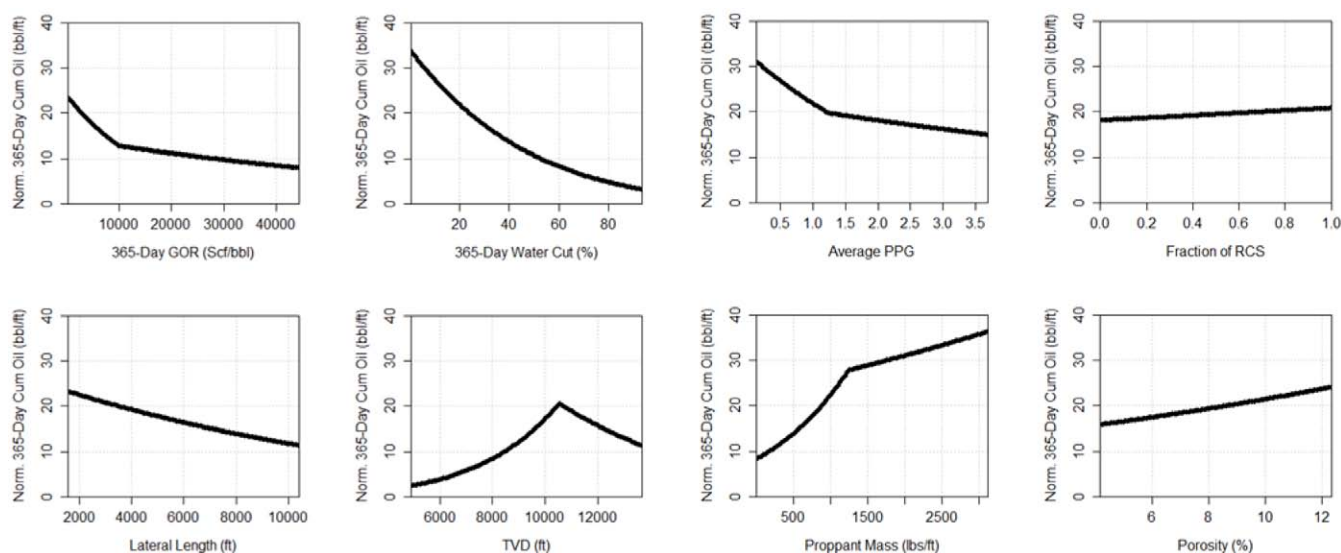


Figure 21—Marginal effect of each predictor in the model on the normalized 365-day cumulative oil production when other predictor variables are held fixed at their mean values.

Fig. 22 shows the variable importance or tornado plot for the ACE model. To identify which predictor variables are statistically most important in the model, we looked for the predictor variable that is associated with the greatest increase in R^2 when that predictor is added to the model that already contains all the other predictors. The model shows that the 365-day water cut is the most influencing reservoir parameter (higher water cut means less oil production), while the proppant mass is the most important completion parameter. Other parameters in decreasing order along with positive or negative proportionality are as follows: GOR (negative), true vertical depth or TVD (positive to about 10,500 ft, then negative), lateral length (negative), average proppant concentration (negative), porosity (positive), and fraction of resin coated sand or RCS (positive). Note that the fraction of RCS is the least significant parameter and it should have a minor impact on the 365-day cumulative oil production. This is also confirmed from the physics-based modeling in the previous section (Fig. 19) where the type of proppant (e.g., enhanced fracture conductivity) was shown to have an insignificant impact on the production response.

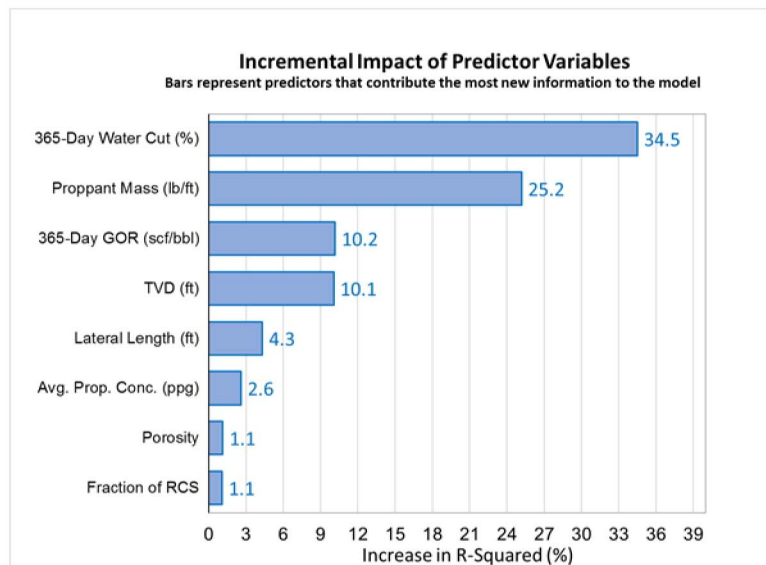


Figure 22—Variable importance for the Turner wells. The two most influencing predictors in the model are the 365-day water cut and proppant mass, followed by GOR and TVD.

Reconciliation of Fracture/Reservoir Modeling and Statistical Analysis

This section compares the detailed single well modeling to the big picture statistical analysis when it comes to predicting the relative increase in production on increasing the treatment size. Fig. 23 compares the relative increase in 365-day cumulative oil production (bbl/ft) with increasing proppant loading from 500 lb/ft as predicted by the detailed fracture/reservoir modeling shown in Fig. 17 (blue) and the ACE MVA (orange). Both models agree reasonably well in predicting the change in oil production as a function of proppant loading, thus, increasing the confidence in the results of this study since the detailed physics-based modeling is consistent with big data analytics. This agreement also provides basis for scaling the results from the single well modeling to the AOI as a whole.

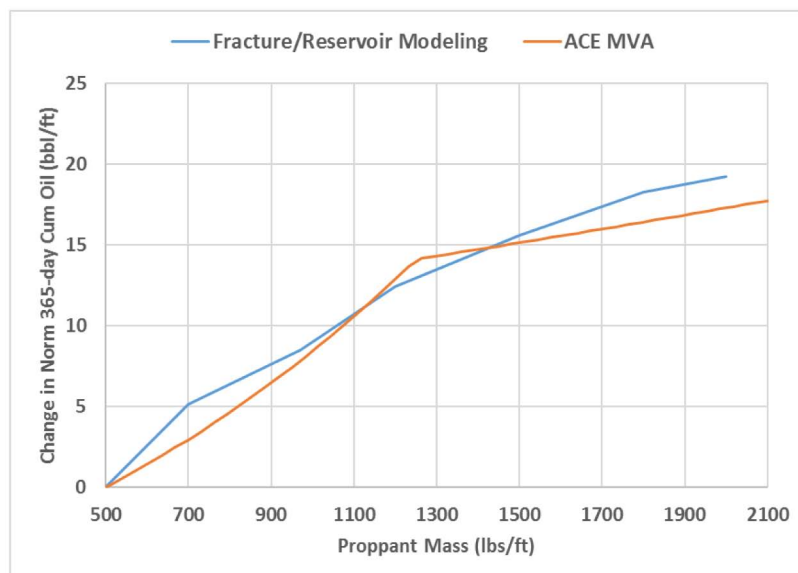


Figure 23—Comparison of detailed fracture/reservoir modeling to ACE MVA in predicting the sensitivity of normalized 365-day cumulative oil production to proppant loading.

Conclusions

1. DFITs in the Turner Formation show an average fracture gradient of 0.71 psi/ft and an average closure pressure gradient of 0.62 psi/ft. The average pore pressure gradient is 0.59 psi/ft.
2. Fracture modeling indicates propped fracture half-lengths of 400 to 600 ft and propped heights of 100 to 240 ft, showing some but not excessive out-of-zone height growth when utilizing a single-entry point design with 100 klb of proppant and 1,200 bbl of 25# crosslinked gel pumped at 15-30 bpm. The fracture conductivity was fairly high at about 300 mD-ft (or equivalent to an F_{cD} of 67).
3. When the proppant loading is held constant at 970 lb/ft and the history matched reservoir permeability is 0.009 mD, numerical reservoir modeling shows that there appears to be no short-term benefit (one-year production) to decreasing the fracture spacing below 120 ft. This occurs because at reduced fracture spacing, both the fracture length and conductivity decrease when the proppant loading is fixed. Also, the current sleeve or cluster spacing of 120 to 180 ft seems to be optimal based on the long-term production forecasts (10 years).
4. When the fracture spacing is held constant at 120 ft, increasing the proppant loading from 970 to 1,800 lb/ft would provide significant short- and long-term production benefits. There appears to be only a slight incremental gain in oil production above 1,800 lb/ft of proppant loading. Thus, the economic benefits of increasing the proppant loading from the current design (970 lb/ft) to 1,800 lb/ft look very attractive, but, would need detailed economic evaluation.
5. For the pump rate sensitivity, the fracture modeling shows that fracture length does not increase substantially at pump rates of 40 bpm or higher when the proppant loading is held constant.
6. The numerical production model shows similar production results using 20/40 PRC, 30/50 Ceramic, and 20/40 Ceramic proppants, thus indicating no production uplift with ceramic proppants. The treatments using any of these proppant types and sizes should yield high dimensionless conductivity fractures of 20 or higher at 0.009 mD reservoir permeability. ACE MVA showed a similar result where the fraction of RCS was found to be least significant parameter.
7. Independent fracture/reservoir modeling and big picture statistics (ACE MVA) showed consistent results in quantitatively predicting the relative increase in 365-day cumulative oil production with increasing proppant loading which is the dominant completion parameter impacting oil production.

Acknowledgments

The authors would thank the management of Ballard Petroleum, LLC for permission to publish this paper and acknowledge their colleagues for their insightful discussions and contributions.

Nomenclature

- F_{cD} = dimensionless conductivity, unitless
 h_f = fracture height, ft
 k = reservoir permeability, mD
 k_f = hydraulic fracture permeability, mD
 w_f = fracture width, inch
 x_f = hydraulic fracture half-length, ft

Abbreviations

- LT 21-7TH = Leavitt Trust 21-7TH (API: 49-005-61485)
 LT 14-2TH = Leavitt Trust 14-2TH (API: 49-005-61487)
 LT 41-34TH = Leavitt Trust Federal 41-34TH (API: 49-005-61894)
 D24-30TH = Dilts Federal 24-30TH (API: 49-005-62329)

D41-24TH = Dilts 41-24TH (API: 49-005-62347)
 D44-15TH = Dilts 44-15TH (API: 49-005-62791)
 R11-10TH = Reno 11-10TH (API: 49-005-62463)
 R42-5TH = Reno 42-5TH (API: 49-005-62449)
 R44-24-1XTH = Roush Federal 44-24-1X TH (API: 49-005-62791)

SI Metric Conversion Factors

acre	x 4.046 873	e+03 = m ²
bbl	x 1.589 874	e-01 = m ³
cp	x 1.0	e-03 = Pa.s
ft	x 3.048	e-01 = m
°F	(°F – 32)/1.8	= °C
lbm/gal	x 1.198 264	e+02 = kg/cm ²
psi	x 6.894 757	e+00 = kPa

References

- Al-Muntasheri, G.A. 2014. A Critical Review of Hydraulic Fracturing Fluids over the Last Decade. Presented at the SPE Western North American and Rocky Mountains Joint Regional Meeting, Denver, Colorado, 16-18 April. SPE-169552-MS.
- Anna, L.O. 2009. Geologic Assessment of Undiscovered Oil and Gas in the Powder River Province, Wyoming and Montana. U.S. Geological Survey Digital Data Series DDS-69-U. p. 55.
- Dolton, G. L. and Fox, J.E. 1996. Powder River Basin Province (033), in Gautier, D.L., Dolton, G.L., Varnes, K.L., and Takahashi, K.I., eds., 1995 *National Assessment of United States Oil and Gas Resources—Results, methodology, and supporting data: U.S. Geological Survey Digital Data Series DDS-30, one CD-ROM, Release 2*.
- Gonzales, D., Costello, D., and Loxton, G. 2017. History Match Case Study of a Multi PVT Fluid Regime in an Unconventional Tight Sand Reservoir Located in the Powder River Basin. Presented at the SPE Eastern Regional Meeting, Lexington, Kentucky, 4-6 October. SPE-187534-MS.
- Gonzales, V.M., et al. 2012. Understanding Production Drivers and Challenges in Converting a Vertical to Horizontal Oil Play Utilizing Single Well Modeling. Presented at the SPE Canadian Unconventional Resources Conference, Calgary, Alberta, Canada, 30 October-1 November. SPE-161771-MS.
- Ingle, T., et al. 2017. Practical Completion Design Optimization in the Powder River Basin—An Operator Case Study. Presented at the SPE Unconventional Resources Conference, Calgary, Alberta, Canada, 15-16 February. SPE-185064-MS.
- Le, T. et al. 2018. Integrated Stratigraphic Controls for Flow Simulation of the Wall Creek Member in the Frontier Formation: Western Powder River Basin, Wyoming. Presented at the SPE Western Regional Meeting, Garden Grove, California, 22-27 April. SPE-190095-MS.
- Lolon, E. et al. 2018. Augmenting Hybrid Physics-Based Multivariate Analysis with the Alternating Conditional Expectations Approach to Optimize Permian Basin Well Performance. Presented at the SPE Liquids-Rich Basins Conference—North America, Midland, Texas, 5-6 September. SPE-191798-MS.
- Olaoye, O., et al. 2016. Evaluating the Application of Unconventional Resource Extraction Technology to a Conventional Play. Presented at the SPE Liquids-Rich Basins Conference—North America, Midland, Texas, 21-22 September. SPE-182502-MS.
- Ruhle, W. and Orth, J. 2015. Production Trends from the Exploitation of Horizontal Completions in the Upper Cretaceous Formations of the Powder River Basin: A Look Back on Five Years of Development. Presented at the SPE/CSUR Unconventional Resources Conference, Calgary, Alberta, Canada, 20-22 October. SPE-175957-MS.